Drug Development and Industrial Pharmacy, 34:974–983, 2008

ISSN: 0363-9045 print / 1520-5762 online
DOI: 10.1080/03639040802149087

informa
healthcare

The Influence of Crystal Habit on the Prediction of Dry Powder Inhalation Formulation Performance Using the Cohesive–Adhesive Force Balance Approach

Jennifer C. Hooton, Matthew D. Jones, Haggis Harris, Jagdeep Shur, and Robert Price

Pharmaceutical Surface Science Research Group, Department of Pharmacy and Pharmacology, University of Bath, Bath, UK

The aim of this investigation was to study the influence of crystalline habit of active pharmaceutical ingredients on the cohesive–adhesive force balance within model dry powder inhaler (DPI) formulations and the corresponding affect on DPI formulation performance. The cohesive–adhesive balance (CAB) approach to colloid probe atomic force microscopy (AFM) was employed to determine the cohesive and adhesive interactions of micronized budesonide particles against the {102} and {002} faces of budesonide single crystals and crystalline substrates of different sugars (cyclodextrin, lactose, trehalose, raffinose, and xylitol), respectively. These data were used to measure the relative level of cohesion and adhesion via CAB and the possible influence on in vitro performance of a carrier-based DPI formulation. Varying the crystal habit of the drug had a significant effect on the cohesive measurement of micronized budesonide probes, with the cohesive values on the {102} faces being approximately twice that on the {002} crystal faces. However, although different CAB values were measured with the sugars with respect to the crystal faces chosen for the cohesive-based measurement, the overall influence on the rank order of the CAB values was not directly influenced. For these data sets, the CAB gradient indicated that a decrease in the dominance of the adhesive forces led to a concomitant increase in fine particle delivery, reaching a plateau as the cohesive forces became dominant. The study suggested that crystal habit of the primary drug crystals influences the cohesive interactions and the resulting force balance measurements of colloid probe CAB analysis.

Keywords CAB; atomic force microscopy; budesonide; crystal face

INTRODUCTION

The use of dry powder inhaler (DPI) formulations for drug delivery via the respiratory tract is well established and provides several key advantages over other forms of respiratory drug delivery (Harjunen, Lankinen, Salonen, Lehto, & Jarvinen, 2003; Steckel & Bolzen, 2004; Zeng, Martin, & Marriott, 1995; Zeng, Martin, Marriott, & Pritchard 2000a, 2000b). Typically, DPI formulations are comprised of coarse carrier particles (traditionally α-lactose monohydrate) processed with micronized drug via low- or high-shear blending processes. The blending of drug and carrier not only improves the flowability and content uniformity of the drug within the formulation, but promotes the fluidization and aerosolization of the formulation from the device into the air stream during inhalation.

Although lactose has been the excipient of choice for three decades, there have recently been concerns regarding its suitability. Lactose is a reducing sugar and may lead to chemical instability particularly in formulations involving protein and peptides (Kretchmer, 1972). In addition, recent concerns regarding *transmissible spongiform encephalopathies* (TSE) via residual calf rennet protein have raised issues relating to the potential of such contamination (Steckel & Bolzen, 2004). Thus, the possibility for the use of an alternative nonreducing and nonbovine carbohydrate carrier and/or a selection of such carriers may have considerable benefits. Although several studies have shown the potential for the use of alternative sugars as carriers (Cline & Dalby, 2002; Steckel & Bolzen, 2004; Tee, Marriott, Zeng, & Martin, 2000), there has been very little scientific-based understanding in examining the underlying interfacial properties between drug and carrier, and how it may be possible to judiciously select drug-excipient combinations in relation to the design and energy requirements of a particular DPI device.

To investigate the underlying mechanism of interaction between drug and excipient, the atomic force microscopy (AFM) has been used to measure the interfacial force balance between an active pharmaceutical ingredient (API) and substrate surfaces via the cohesive–adhesive balance (CAB) approach (Begat, Morton, Staniforth, & Price, 2004). In a previous study, it was shown that by applying the CAB technique to a

Address correspondence to Robert Price, Pharmaceutical Surface Science Research Group, Department of Pharmacy and Pharmacology, University of Bath, Bath BA2 7AY, UK. E-mail: r.price@bath.ac.uk

model drug (salbutamol sulfate) and a range of different sugars, it was possible to derive a correlation between the force balance of different drug–sugar combinations determined from the CAB data and in vitro formulation performance (Hooton, Jones, & Price, 2006).

One of the many concerns in the processing of drug actives for DPI formulations is the influence of the physicochemical properties of the input material on product functionality. Furthermore, the relationship between the characteristic properties of the unprocessed drug material (e.g., crystalline habit, residual solvents, and mechanical properties) upon secondary processed (e.g., micronized) material is also not widely understood.

The crystal habit of the unprocessed active ingredient, for example, is known to be affected by many factors, including the kinetics of crystal growth relating to levels of supersaturation, level of impurities, crystallization process parameters (e.g., stirrer speed) and the solvents and/or antisolvents utilized in crystallization (Blagden et al., 1998; Mullin, 2001; Wells, 1946). Thus, changing the crystallization conditions of an API may effect the growth rates of different crystal faces, which may lead to a change in the crystal habit in relation to the dominance of the slowest growing face. This may subsequently modify the interfacial properties (e.g., surface free energy, Young's modulus) of the crystal due to a change in the orientation of the different chemical groups on the respective growth faces. Muster and Prestidge (2002) have demonstrated the influence of molecule orientation at crystal faces on the surface free energy and interfacial interactions of model hydrophobic silica particles. The study highlighted the importance of crystal-face-specific properties and their possible implications on processing, formulation, and delivery of APIs.

In this study, the use of the CAB approach to predict formulation performance characteristics of DPI formulations has been extended to study the effects of different crystal faces on the cohesive interactions of a micronized drug. In this study, budesonide—a hydrophobic corticosteroid—was crystallized using two different solvents, which led to the dominance of two different crystalline habits. Force measurements were performed against the dominant faces of these two habits to generate two sets of cohesive data, which were both employed for the subsequent CAB analysis with different sugars.

METHODS

Materials

Micronized budesonide was obtained from Sicor (Batch number 6157/MI, Santhia, Italy). The sugars used were xylitol (CM90, BN H029 34220, Danisco Sweeteners, Kantvik, Finland), α,α-trehalose dihydrate (BN 1J271, British Sugar, Peterborough, UK), D-raffinose pentahydrate (BN 04805BA, Sigma, Poole, UK), α-lactose monohydrate (Lactochem, BN D017194, Domo, Borculo, Netherlands), and β-cyclodextrin (Cavitron 82900, Cerestar Inc, Hammond, IN, USA). Ethanol and acetonitrile were obtained from Fisher chemicals (Fisher Chemicals, Loughborough, UK), and *N*, *N*-dimethyl formamide was obtained from Aldrich (Aldrich, Gillingham, UK). Ultrapure water was obtained via reverse osmosis (MilliQ, Millipore, Molsheim, France).

Preparation of Crystal Substrates

In order to perform quantitative CAB analysis, single crystals of budesonide and excipient materials were produced using an antisolvent technique (Hooton et al., 2006). Briefly, saturated solutions of the excipients were produced using 10 mL of water as the solvent. The resulting solutions were sonicated for 10 min and then left to stand for 1 h before being filtered through a polytetrafluoroethylene (PTFE) filter of 0.2-mm pore size (Whatman, Brentford, UK). Approximately 0.5 mL of the resulting saturated solution was placed on a microscope coverslip, which in turn was placed upon a supporting pillar in a vessel containing the antisolvent. A second vessel was then placed over the pillar in order to create an enclosed environment allowing the diffusion of the antisolvent vapor to induce nucleation and crystal growth. The heterogeneous nucleation and crystal growth of the crystals to the glass surface of the coverslip acted as the substrates for AFM studies without any requirement for manipulation and handling.

Similarly, single budesonide crystals were also produced using the same technique, although different solvent and antisolvent combinations were used to produce the two distinct crystalline habits. The two solvents used were *N*, *N*-dimethylformamide (DMF) and ethanol with water as the antisolvent in both studies. Preliminary, crystallization studies suggested that two distinct crystalline habits could reproducibly be formed using the two different solvent/antisolvent combinations.

A computer crystal structure simulation program (SHAPE V7.0, Shape Software, Kingsport, USA) was used to model the crystal habit and to characterize the Miller indices of the growth faces of the budesonide crystals formed. A budesonide structural model (EPSRC Chemical Database Service, Daresbury, UK) based on single crystal X-ray diffraction data (Albertsson, Oskarsson, & Svensson, 1978) was subsequently used to model the molecular orientation at the various crystal faces and the functional groups of the respective surfaces via a crystallographic software package (MS Modelling v3.2.0.0, Accelrys Software Inc., Cambridge, UK).

The dominant faces of the crystals produced were analyzed by AFM imaging to ensure that the surfaces possessed adequately smooth surfaces for CAB measurements. All topographical measurements were undertaken with a NanoScope IIIa MultiMode AFM in TappingMode™ operation (all Digitial Instruments, Santa Barbara, CA, USA). A TESP Olympus tip (Digital Instruments, Cambridge, UK) was used to image a 5-μm square region of the surface at a scan rate of 1 Hz. From the resulting image, the root-mean-square (R_q) roughness was determined using the in-built software.

Preparation of Probes and Performance of AFM Measurements

Individual micronized particles of budesonide were mounted onto the apex of tipless cantilevers (DNP-020, Digital Instruments) with a nominal spring constant (k = 0.58 N/m), as described previously (Begat et al., 2004). Force volume measurements were subsequently performed against the smooth substrates of the dominant faces of budesonide crystals and the respective sugars (Hooton et al., 2006). In the force volume mode, the AFM raster scans the substrate under the colloidal probe to produce a series of force curves, each from a well-defined location in the x and y direction. These data can be processed to calculate the force of adhesion from each individual force curve, which can be displayed as a lateral and spatially resolved force map, showing variation in adhesion over the surface. The adhesion data obtained from the sugar substrates were subsequently plotted against the cohesive measurements to obtain the respective CAB ratios for the different crystal habits of the drug substrates.

Processing and In Vitro Testing of Carrier-Based DPI Formulations

Particle Size Analysis

The particle size distributions of budesonide and excipient materials were determined by laser light scattering (Mastersizer X, Malvern Instruments, Malvern, UK) using a small volume circulating sample dispersion cell. Approximately 100 mg of powder was suspended in a 0.1% (wt/wt) lecithin cyclohexane solution and sonicated for 5 min at 25°C prior to analysis. Cumulative undersize particle diameters were calculated and corrected for refractive index using best-fit algorithm software. All samples were prepared and analyzed in triplicate.

Particle size analysis of micronized budesonide determined a median equivalent volume diameter of 3.24 ± 0.24 μm, with 90% of particles under 5.0 μm. Hence, the active was suitable for delivery to the lungs. The 63–90 μm sieve fraction of the sugars was used as coarse carriers for the budesonide formulations (Hooton et al., 2006). The particle size data indicated that the only significant ($p > .05$) difference in fines was between lactose and cyclodextrin. Significant differences in median particle size (d = 0.5) were determined between lactose and xylitol, raffinose and β-cyclodextrin, and trehalose and β-cyclodextrin.

Scanning Electron Microscopy

Scanning electron microscopy (SEM) (Jeol 6310, Jeol, Tokyo, Japan) analysis was undertaken of both the raw materials and the blends in order to provide visual characterization of any changes that may have resulted from the blending and storage process. The samples were sputter coated with a thin gold film prior to imaging (Model S150B, Edwards high vacuum, Sussex, UK).

Production of DPI Formulation Blends

Carrier-based DPI blends, consisting of a 200-μg budesonide dose per 33 mg of the formulation, were produced using a low-shear blending process, as described previously (Hooton et al., 2006). Briefly, the coarse carrier was added geometrically to the drug, with the formulation being mixed with a Whirlimixer (Fisons Scientific Apparatus, Loughborough, UK) for 45 s between each addition. Once the total quantity of carrier was added, the formulation was placed in a Turbula blender (Type T2F, Bachofen AG, Basel, Switzerland) operating at 46 revolutions per minute for 40 min.

High-Performance Liquid Chromatography and Content Uniformity Analysis of Budesonide

Drug content was analyzed using a validated high-performance liquid chromatography (HPLC) methodology. The HPLC assay consisted of a pump (Jasco PU-980, Jasco Corp., Tokyo, Japan), connected to a Hypersil column (Hypersil MOS C8, 5 μm, 4.6 × 100 mm, Jones Chromatography Ltd, Hengoed, UK) operated at room temperature, which in turn was coupled to a UV detector set at 248 nm. The mobile phase flow rate was 1.5 mL/min, and the injection volume was 100 μL. The total running time per injection was 6 min, with a retention time of approximately 4 min. A budesonide trace consisted of two peaks, corresponding to the 22R- and 22S-enantiomers of budesonide.

The drug content uniformity of the blends was determined by taking 10 random samples of 33 ± 1 mg from the processed blend and dissolving in 50 mL of a mobile phase (60:40 water:acetonitrile). HPLC was then used to determine the drug concentrations for the drug content uniformity measurements. The proportion of drug in each sample was calculated and the content uniformity expressed by percentage relative standard deviation. Following content uniformity measurements, 33 ± 1 mg of each blend was loaded into type 3 gelatin capsules and stored at 44% RH for a minimum of 24 h prior to in vitro testing.

In Vitro Inhalation Performance Analysis of Prepared Blends

In vitro deposition measurements were determined using an Andersen Cascade Impactor (ACI) (Copley Scientific Ltd, Nottingham, UK) with a pre-separator containing 10 mL of the mobile phase. Each impactor stage plate was coated with a silicone spray (Dow Corning, Barry, UK). At the flow rate of 60 ± 1 L/min, a total of 5 L of air was drawn through the ACI for each study.

For each experiment, 10 individual capsules of the same formulation were discharged into the ACI at 60 L/min for 5 s via a Cyclohaler (Miat SpA, Milan, Italy) DPI device. Following aerosolization, the ACI apparatus was dismantled and the inhaler, capsules, and each part of the ACI were washed down into known volumes of HPLC mobile phase.

The mass of drug deposited on each part of the ACI was determined by HPLC. This protocol was repeated three times for each blend, following which, the mass median aerodynamic diameter (MMAD), geometric standard deviation (GSD), loaded dose, emitted dose, fine particle dose (FPD), and fine particle fraction of the loaded dose (FPF_{LD}) were determined. The FPD represented the mass of drug that was collected on stages 3–8 of the ACI.

RESULTS

Characterization of the Chemical Specificity of the Growth Faces of Budesonide Single Crystals

The dominant growth faces of the excipients used in the generation of CAB data have been previously discussed (Hooton et al., 2006). Budesonide crystals were shown to exhibit different crystal habits dependant on the solvent used for crystallization, without affecting crystal form.

The different crystal habits of the budesonide crystals grown are illustrated in Figure 1. Crystals grown from DMF are dominated by {102} faces. For crystals grown from ethanol solutions, the habit is dominated by {002} faces. The symmetrical nature of the budesonide crystals precluded the specific characterization of the Miller index of the face. However, the same crystal face was used for all force measurements.

Molecular modeling of the surface chemistry of the dominant growth faces of {002} and {102} are shown in Figures 2 and 3, respectively. The {002} faces are dominated by C-H groups. Although there are some C–O–C groups present, these are not located in regions that are readily presented on the surface. There are four possible faces of {102} that could be present on the surface. The (102) and $(\bar{1}0\bar{2})$ faces are similar as both consist of C-H groups as well as some C=O and O-H groups. In contrast, the $(10\bar{2})$ and $(\bar{1}02)$ faces are C-H dominated, but with much larger C–O–C and C=O group contributions.

The crystal modeling of the {002} family of faces shows a surface chemistry that is dominated by hydrophobic, C-H groups. In contrast, the {102} family shows an increased contribution of oxygen molecules. Therefore, the groups associated with {102} have the potential to act as acceptors. In contrast, {002} has no potential to act as either an acceptor or donor. Thus, the {102} surface would have the potential to form apolar and polar contributions to the van der Waals force of interaction, whereas the {002} would only be able to adhere via apolar-based interactions.

Whereas the {102} face has the potential for asymmetric polar interactions, the potential of a micronized budesonide particle to act as either a donor or acceptor is unknown, as it is not possible to determine the chemistry of fractured surfaces. Should the face of budesonide display a dominance of donor groups, then the resulting difference in behavior may lead to changes in the cohesive behavior between these crystal substrates.

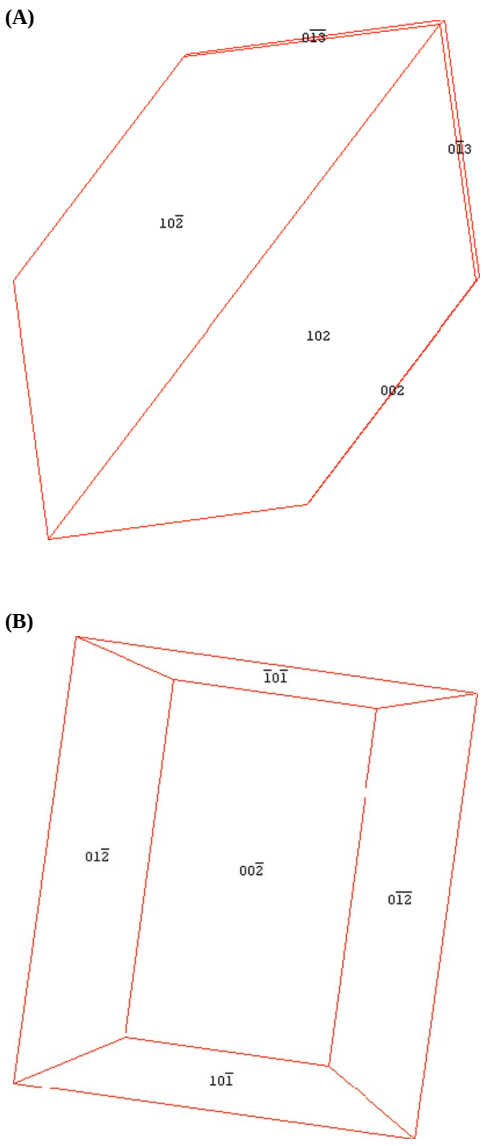

FIGURE 1. The crystal habits of budesonide crystals grown from (A) *N*, *N*-dimethylformamide that exhibit the dominant {102} face and (B) ethanol solutions that exhibit the dominant {002} face.

The Influence of Drug Substrate Surface Chemistry on the Cohesive–Adhesive Balance of Micronized Budesonide

The cohesive force data acquired for the interaction of micronized budesonide probes on the {102} and {002} faces of the budesonide crystals were plotted as a function of the adhesive interactions of the same micronized budesonide probes against the various sugars, and are summarized in Figures 4A–E and summarized in Table 1

For the same set of colloid probes, micronized budesonide probes were most adhesive to the xylitol substrate. For the interaction of micronized budesonide probes with xylitol and the {102} face of budesonide, the force of adhesion (F_{adh}) was

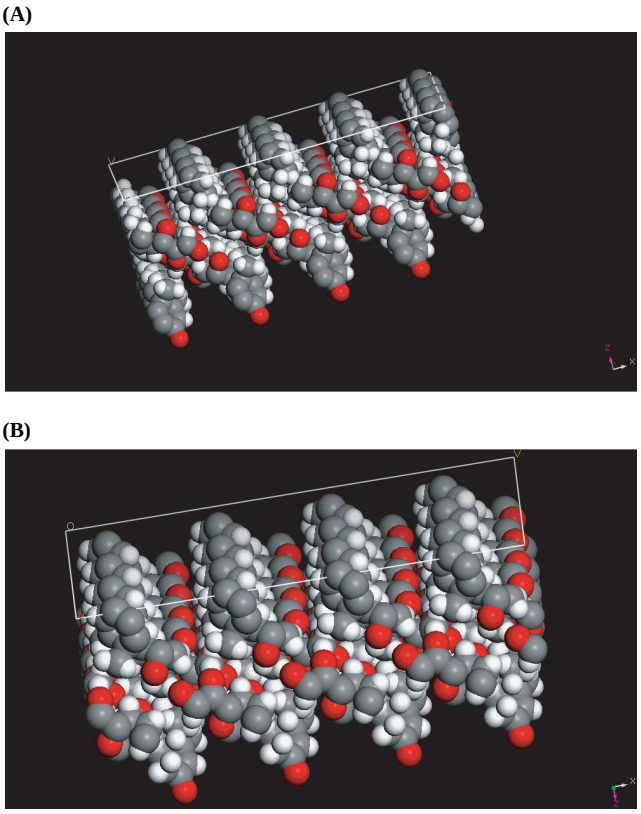

FIGURE 2. Modeling of the {002} family of crystal faces (A) (002) crystal face of budesonide and (B) $(00\bar{2})$crystal face of budesonide.

1.33 times greater than the cohesive interaction (F_{coh}). For the {002} face, the F_{adh} of the budesonide probes to the xylitol substrate was 2.91 times greater than the cohesive interaction of budesonide. These data further suggested that the cohesive interaction of micronized budesonide on the {102} face was over two times greater than that on the {002} face.

The micronized budesonide probes also indicated a greater propensity to adhere to the trehalose and raffinose crystals than the {102} and {002} faces of the budesonide crystals. The adhesive interaction to trehalose was 1.22 times greater than the cohesive interaction with the {102} face and 2.75 times greater with respect to the cohesive interaction with the {002} face. For raffinose, the adhesive interaction was 1.13 times more dominant than the cohesive interaction with {102}. However, with respect to the cohesive interactions of the micronized drug with the {002} face, the adhesive interaction against raffinose was 2.46 times greater.

For the interaction of micronized budesonide with the {102} budesonide substrate and lactose, two of the three probes indicated a slight dominance of the adhesive interaction, whereas for the other probe the cohesive interaction dominated. These data indicated that the force balance was around the equilibrium value, with the $F_{coh} = 1.19F_{ad}$ ($R^2 = 0.95$). Meanwhile, the interaction of micronized budesonide with the {002} face and lactose was dominated by the adhesive interaction, with the budesonide–lactose interaction being approximately twice ($F_{coh} = 0.54\ F_{ad}$ [$R^2 = 0.98$]) as adhesive as the interaction with the {002} face.

Cyclodextrin was the only substrate to show cohesive interactions for the two single crystal substrate surfaces of budesonide. For the {102} and {002} face, there is a strong cohesive tendency with the $F_{coh} = 11.42\ F_{ad}$ ($R^2 = 0.83$) and $F_{coh} = 5.32\ F_{ad}$ ($R^2 = 0.95$), respectively.

These data suggest that the crystallization process and the surface chemistry of the unprocessed drug crystals may have a significant influence on the subsequent processing of the active. The CAB measurements indicated that the interaction of the micronized budesonide probes used in this study are significantly weaker on the {002} than the {102} family of faces.

It is of interest to note that the rank order of the adhesive behavior of budesonide has changed with respect to previous work on the interaction of salbutamol sulfate with the various carbohydrates (Hooton et al., 2006). These data suggest that the relationship between drug–drug and drug-excipient interactions is highly dependent on both physical and chemical characteristics of the raw and processed materials.

In Vitro Performance of Carrier-Based Formulations of Budesonide and the Excipients

The in vitro impactor performance data and content uniformity measurements of the various budesonide-excipient blends are shown in Table 2. In addition, Figure 5 shows electron micrographs of each of the carriers employed in the study. Whereas all sugars gave an acceptable coefficient of variation (CV) of less than 5%, it is interesting to note that the CV of cyclodextrin was higher than the other formulations. A general trend was observed between the fine particle fraction of the loaded dose (%FPF_{LD}) and the efficiency of drug removal from the device. The %FPF_{LD} performance was shown to increase with decreasing amount of drug emitted from the inhaler device. As shown previously, while the emitted dose as a percentage of the total loaded dose of the drug from the xylitol formulations was significantly greater than all other formulations, the %FPF_{LD} was extremely poor and significantly ($p < .005$) lower than other sugars. These data suggest that the elutriation efficiency of the budesonide particles from the surface of xylitol was low. The highest fine particle fraction was measured for the cyclodextrin blend (%FPF_{LD} = 17.01 ± 1.15%) followed by lactose (%FPF_{LD} = 13.24 ± 1.68%), raffinose (%FPF_{LD} = 8.16 ± 2.04%), and trehalose (%FPF_{LD} = 3.83 ± 0.9%) formulations. One-way ANOVA analysis demonstrated that the %FPF_{LD} of all the blends were significantly different ($p < .05$).

DISCUSSION

The advent of the CAB approach for the analysis of colloidal probe force measurements has provided a fundamental

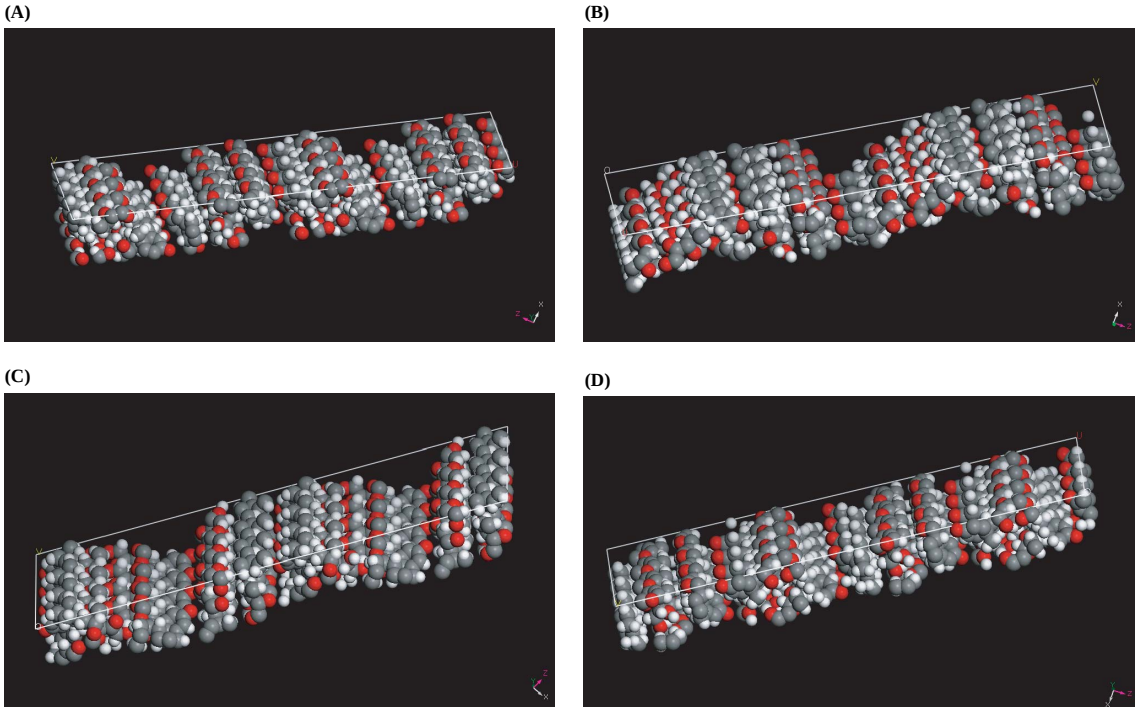

FIGURE 3. Modeling of the {102} family of crystal faces (A) (102), face of budesonide (B) $(10\bar{2})$, face of budesonide (C) $(\bar{1}02)$, face of budesonide, and (D) $(\bar{1}0\bar{2})$face of budesonide.

insight into the interfacial interactions, which may influence the balance of forces within carrier-based DPI formulations (Begat et al., 2004; Hooton et al., 2006).

One of the major concerns of this approach, however, is the need to judiciously select a specific crystal habit of the model drug substrate for cohesive measurements. It is conceivable, therefore, that possible variations in the physicochemical properties of a particular crystal face may significantly influence the force balance, which would concomitantly limit the modeling of the functionality of the API within a carrier-based formulation. One possible means of overcoming such a limitation is to directly measure the cohesive interactions on the crystalline material which is fed into the micronizer, or via characterization of the dominant growth face of the unprocessed drug for single crystal preparation. A representative scanning electron micrograph of as-supplied, unmicronized budesonide material is shown in Figure 6. The crystalline material is dominated by the {102} faces, as obtained via controlled crystallization in *N*,*N*-dimethyl formamide (Figure 1A and 2). Unfortunately, the surface roughness variations and high percentage of intrinsic fines precluded the use of these crystals for reproducible CAB measurements.

To highlight the possible importance of crystal habits, this study specifically addressed their influence on the cohesive and resulting force balance measurement within a carrier-based formulation. For the interaction of the micronized budesonide probes with the {102} and {002} crystal faces, the rank order in terms of their adhesive tendency was the same for the crystal faces, with

Xylitol > Trehalose > Raffinose > Lactose > Cyclodextrin

For all measurements, however, the CAB gradient for the interaction of the micronized drug with the {102} face was approximately twice that of the interaction with the {002} face. Modeling the surface chemistry of the {102} face, the increase in the force of cohesion may be due to the presence of acceptor groups on the surface, which may increase the surface free energy and the corresponding thermodynamic work of cohesion or via an increase in capillary forces in relation to the higher affinity of the crystal face to water adsorption.

To highlight the influence of the CAB data on the fluidization and aerosolization performance of the prepared formulation, plots of the percentage emitted dose fraction (%EF) and $\%FPF_{LD}$ as a function of the CAB values for the {102} and {002} crystal faces with the various excipients are shown in Figures 7 and 8, respectively.

The relationship between the cohesive and adhesive balance and the corresponding aerosolization data have not been influenced by measuring the cohesive interactions with either the {102} or {002} faces. The high %EF of the adhesively led

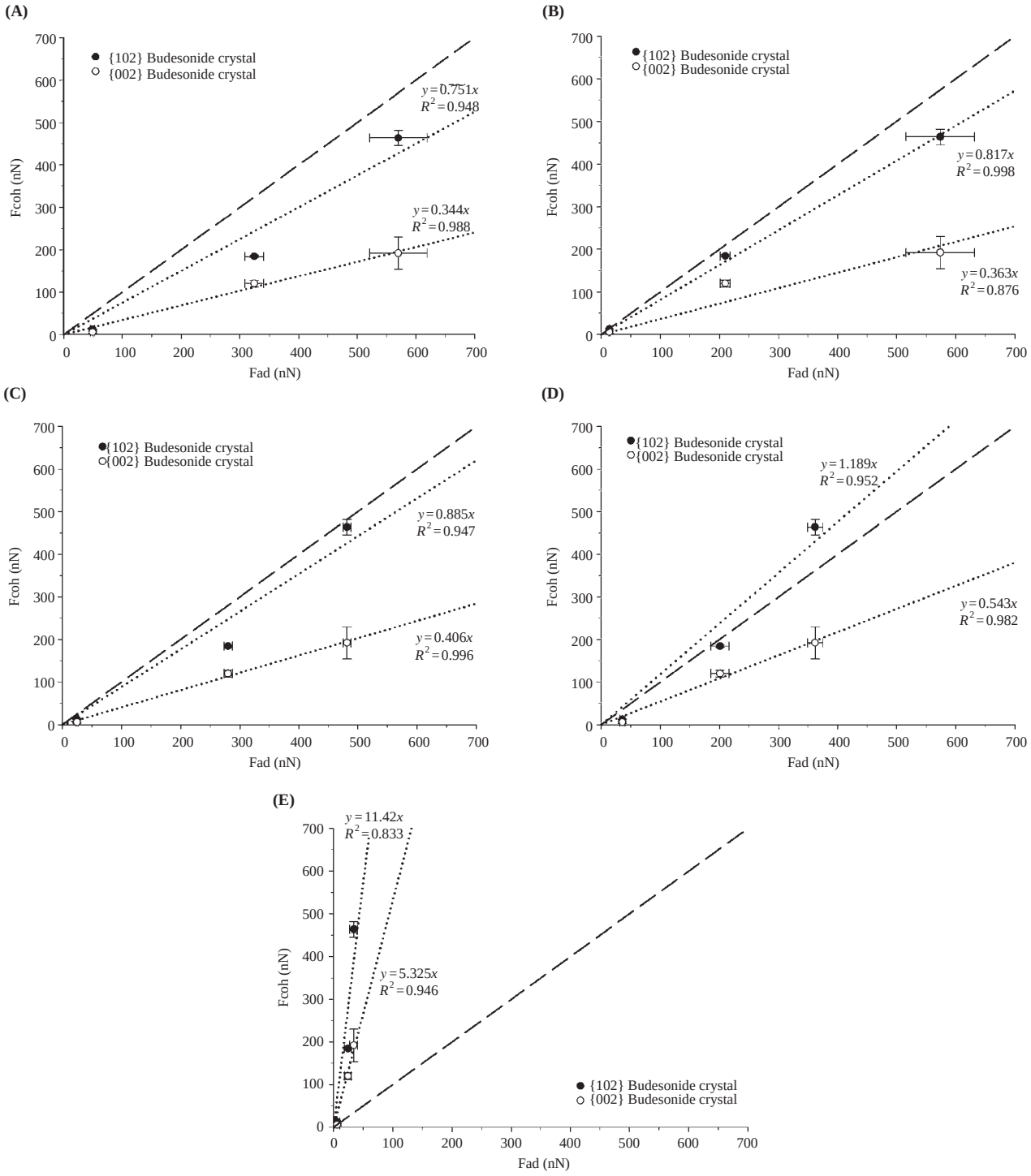

FIGURE 4. Relationship between the force of cohesion on the {102} and {002} and the force adhesion of micronized budesonide probes with (A) xylitol, (B) trehalose, (C) raffinose, (D) lactose, and (E) cyclodextrins via cohesive–adhesive balance (CAB)-based analysis.

systems (CAB ratio < 1) suggests that the degree of drug loss within the inhaler device may be related to the CAB value. These data suggest that the greater the adhesive tendency of the drug with respect to its cohesive interaction, the higher the emitted dose. However, the $\%FPF_{LD}$ versus CAB data in Figure 8 suggests that the greater the tendency of the drug to adhere to the excipient with respect to its cohesive interaction, the lower the $\%FPF_{LD}$ and thus reduces the deaggregation

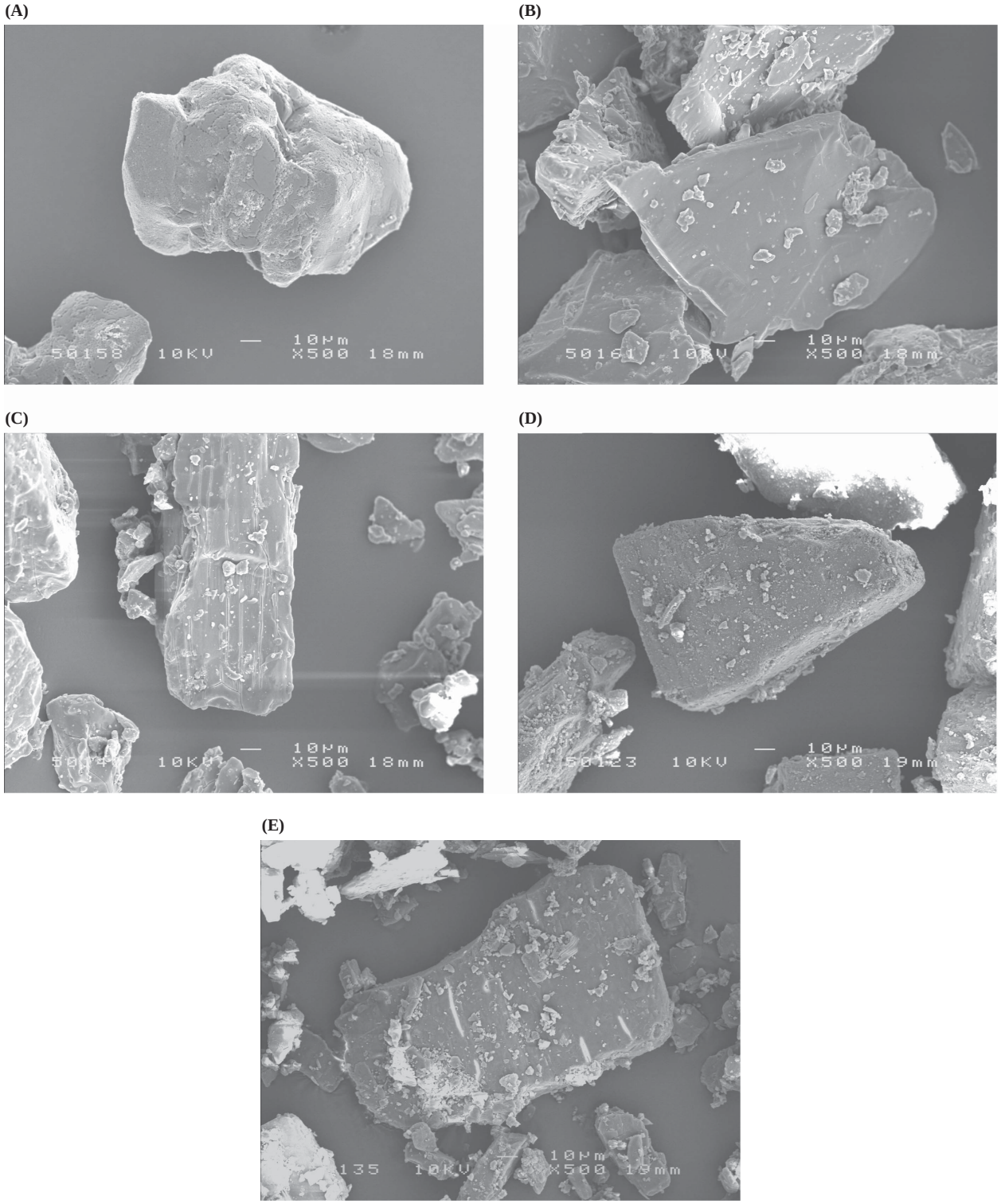

FIGURE 5. Scanning electron micrographs of binary blends of micronized budesonide with (A) xylitol, (B) trehalose, (C) raffinose, (D) lactose, and (E) cyclodextrin.

TABLE 1
The Cohesive–Adhesive Balance (CAB) Ratios of the Interactions of Micronized Budesonide with the {102} and {002} Faces of Budesonide and Various Carrier Sugars

	CAB Ratio	
Sugar Substrate	{102}	{002}
Xylitol	0.751	0.344
Trehalose	0.817	0.363
Raffinose	0.885	0.406
Lactose	1.189	0.543
Cyclodextrin	11.42	5.325

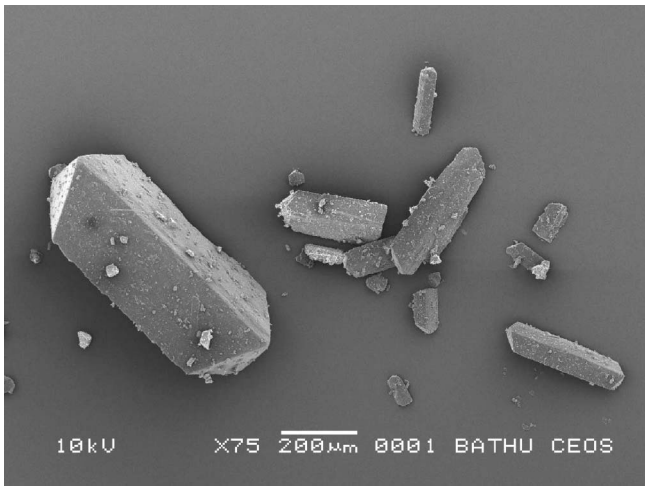

FIGURE 6. Scanning electron micrograph of unprocessed crystalline budesonide obtained via controlled crystallization in *N*,*N*-dimethyl formamide showing the dominant {102} faces.

TABLE 2
Content Uniformity, % Emitted Fraction (%EF, Emitted Dose Expressed a Percentage of Loaded Dose), and Fine Particle Fraction of the Loaded Dose (FPF%) for each of the Sugar Carriers (*SD* in Brackets)

	Content Uniformity (%)	Emitted Fraction (%)	Fine Particle Fraction (%)
Xylitol	2.13	98.36 (0.41)	0.46 (0.06)
Trehalose	1.03	92.94 (0.54)	3.83 (0.90)
Raffinose	1.18	90.12 (1.65)	8.16 (2.04)
Lactose	2.55	82.48 (2.02)	13.24 (1.68)
Cyclodextrin	4.44	77.67 (3.77)	17.01 (1.15)

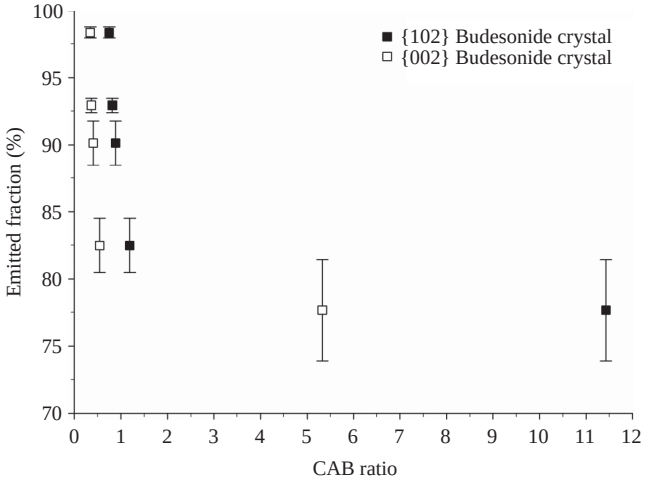

FIGURE 7. Relationship between the emitted dose fraction measurements of micronized budesonide from the various excipients and their respective cohesive–adhesive balance (CAB) ratios.

efficiency of the drug from the excipient surface upon aerosolization.

The CAB data showed that the xylitol was the most adhesively led excipient. This corresponded to the highest emitted fraction of the drug for all the formulations. However, the dominance of the adhesive interaction of budesonide to xylitol corresponded to the lowest $\%FPF_{LD}$. The CAB values for the interaction of micronized budesonide to trehalose and raffinose was higher than xylitol for both the {102} and {002} crystal faces, relating to a significant decrease in the degree of propensity of the drug to adhere to the excipient, although the adhesive interaction remained dominant. The corresponding formulation performance data indicated that this decrease led to higher device retention of the drug with respect to xylitol but a corresponding higher aerosolization efficiency of the drug from the excipient.

Although lactose and cyclodextrin formulations exhibited the lowest %EF, the $\%FPF_{LD}$ of budesonide was significantly higher for these excipients. The highest $\%FPF_{LD}$ was determined for the cyclodextrin formulations which corresponded to a cohesively led system with respect to both the {102} and {002} face of budesonide. The $\%FPF_{RD}$ of the lactose formulations was lower higher than the formulations consisting of the other excipients, but lower than that of the cyclodextrin formulation. This formulation performance trend of the lactose formulation reflects the adhesive tendency of budesonide to lactose with respect to {002} budesonide crystal face. However, measuring the cohesion of the drug on the {102}

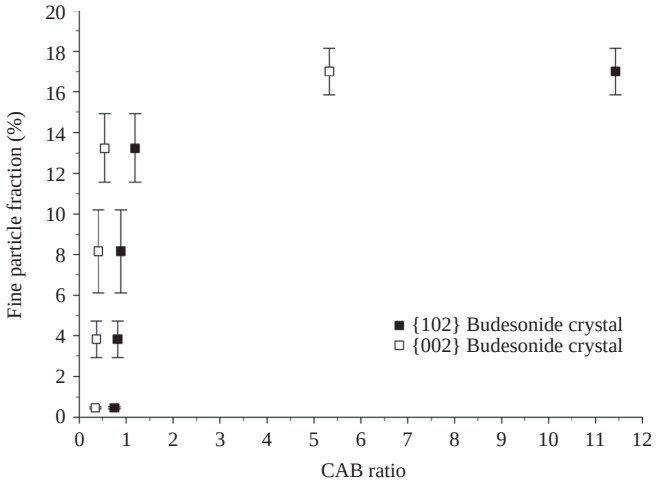

FIGURE 8. Relationship between the fine particle fraction ($\%FPF_{LD}$) measurements of micronized budesonide from the various excipients and their respective cohesive–adhesive balance (CAB) ratios.

face and lactose shifted the force balance toward the force equilibrium where cohesion and adhesion interactions are equivalent.

These data suggest that the dominant growth face of the drug substrate may have a significant effect on the force balance measurements of the drug probes using CAB. Furthermore, these data suggest that the crystalline habit of the primary particles may be important regarding the physicochemical properties of the secondary processed (e.g., micronized) material, which may, therefore, influence the interfacial interactions and aerosol delivery performance of DPI formulations.

CONCLUSIONS

The potential of the CAB-based approach for predicting blend and performance characteristics of DPI formulations has been further demonstrated for budesonide. The study highlighted, however, that the CAB values obtained from AFM-based force measurements are highly dependant on the Miller index plane of the substrate used for the cohesive measurement. Whereas the use of different crystalline faces of budesonide crystals directly influenced the force balance of micronized budesonide, the rank order in the CAB values was not directly affected by varying crystal habits. As shown previously for salbutamol sulfate, the dominance of an adhesive interaction indicated higher device emission efficiencies but a lowering in the fine particle delivery performance.

ACKNOWLEDGMENTS

JCH acknowledges the Engineering and Physical Sciences Research Council for funding.

REFERENCES

Albertsson, J., Oskarsson, A., & Svensson, C. (1978). X-ray study of budesonide: Molecular structure and solid solutions of the (22S) and (22R) epimers of 11 beta, 21-dihydroxy-16alpha-propylmethylenedioxy-1,4-pregnadiene-3,20-dione. *Acta. Cryst. B., 34*, 3027–3036.

Begat, P., Morton, D., Staniforth, J., & Price, R. (2004). The cohesive-adhesive balances in dry powder inhaler formulations I: Direct quantification by atomic force microscopy. *Pharm. Res., 21*(9), 1591–1597.

Blagden, N., Davey, R. J., Lieberman H. F., Williams, L., Payne, R., Roberts, R., Rowe, R., & Docherty, R. (1998). Crystal chemistry and solvent effects in polymorphic systems Sulfathiazole. *J. Chem. Soc., Faraday. Trans., 94*(8), 1035–1044.

Cline, D., & Dalby, R. (2002). Predicting the quality of powders for inhalation from surface energy and area. *Pharm. Res., 19*(9), 1274–1277.

Harjunen, P., Lankinen, T., Salonen, H., Lehto, V., & Jarvinen, K. (2003). Effects of carriers and storage of formulation on the lung deposition of a hydrophobic and hydrophilic drug from a DPI. *Int. J. Pharm., 263*, 151–163.

Hooton, J. C., Jones M. D., & Price, R. (2006). Predicting the behaviour of novel sugar carriers for dry powder inhaler formulations via the use of a cohesive-adhesive force balance approach. *J. Pharm. Sci., 95*(6), 1288–1297.

Kretchmer, N. (1972). Lactose and lactase. *Sci. Am., 227*(4), 74–78.

Mullin, J. W. (2001). *Crystallization* (4th ed.). Oxford: Butterworth-Heinemann.

Muster, T. H., & Prestidge, C. A. (2002). Face specific surface properties of pharmaceutical crystals. *J. Pharm. Sci., 91*(6), 1432–1444.

Steckel, H., & Bolzen, N. (2004). Alternative sugars as potential carriers for dry powder inhalation. *Int. J. Pharm., 270*, 297–306.

Tee, S. K., Marriott, C., Zeng, X. M., & Martin, G. P. (2000). The use of different sugars as fine and coarse carriers for aerosolised salbutamol sulphate. *Int. J. Pharm., 208*, 111–123.

Wells, A. F. (1946). Crystal habit and internal structure. *Philos. Mag., 37*, 184–199.

Zeng, X. M., Martin, G. P., & Marriott, C. (1995). The controlled delivery of drugs to the lung. *Int. J. Pharm., 124*, 149–164.

Zeng, X. M., Martin, G. P., Marriott, C., & Pritchard, J. (2000a). The influence of carrier morphology on drug delivery by dry powder inhalers. *Int. J. Pharm., 200*, 93–106.

Zeng, X. M., Martin, G. P., Marriott. C., & Pritchard, J. (2000b). The effects of carrier size and morphology on the dispersion of salbutamol sulphate after aerosolization at different flow rates. *J. Pharm. Pharmacol., 52*, 1211–1221.